Proceedings World Geothermal Congress 2020+1
Reykjavik, Iceland, April - October 2021

The Acoculco High Temperature Area in Mexico: Resistivity Survey (TEM and MT); Data Acquisition, Processing and Inversion – Geological Significance

Gylfi Páll Hersir[1], Claudia Arango Galván[2], Ásdís Benediktsdóttir[1], Sebastian Held[3], José Manuel Romo Jones[4], Jose Luis Salas[2], Thalia Aviles[4], Diego Ruiz Aquilar[5], Arnar Már Vilhjálmsson[1], Adele Manzella[6] and Alessandro Santilano[6]

[1]Iceland GeoSurvey, Grensásvegi 9, 108 Reykjavík, Iceland.

[2]Universidad Nacional Autónoma de México, Ciudad Universitaria, Delegación Coyoacán, 04510, México CDMX, México

[3]Karlsruhe Institute of Technology, 76131 Karlsruhe, Germany

[4]Centro de Investigación Científica y de Educación Superior de Ensenada, C.P. 22860, Baja California, México

[5]Cátedras Conacyt-Centro de Investigación Científica y de Educación Superior de Ensenada, C.P. 22860, Baja California, México

[6]National Research Council, Institute of Geosciences and Earth Resources, Via G. Moruzzi 1, 56124 Pisa, Italy.

E-mail address: gph@isor.is

Keywords: GEMex, Acoculco, enhanced geothermal system, resistivity, magnetotellurics, transient electromagnetics, geophysical interpretation.

ABSTRACT

GEMex (Cooperation in Geothermal energy research Europe-Mexico for development of Enhanced Geothermal Systems and Superhot Geothermal Systems) is a joint geothermal project of a European and Mexican consortium which began in late 2016 with the purpose to develop geothermal energy in the easternmost region of the Trans-Mexican Volcanic Belt. Two sites that belong to the Comisión Federal de Electricidad (CFE) have been investigated. One of them, the Los Humeros high-temperature area is a superhot geothermal system. The other one, Acoculco high-temperature geothermal area has been proposed to develop an Enhanced Geothermal System (EGS). To characterize an EGS development site in Acoculco, extensive geological, geochemical and geophysical studies were carried out. Already existing regional gravity and magnetic maps were analysed, and gravity was measured on a dense grid. A total of 18 micro-seismic stations were set up which collected data for about a year. Finally, 68 co-located MT and TEM soundings were measured in 2017-2019 through a joint effort by the European and Mexican partners. Their location was based on the interpretation of already existing resistivity measurements as well as a recent geological model of the area. The TEM was measured using TerraTEM equipment and the MT data were collected using instruments from the Metronix manufacturer. The Bounded Influence Remote Reference Processing method (BIRRP) was used for processing the MT time-series. Each TEM/MT pair was jointly inverted in 1D, using the TEM data to static shift correct the MT data.

The authors wish to thank the Comisión Federal de Electricidad (CFE) for their assistance and support. This paper presents results of the GEMex Project, funded by the European Union's Horizon 2020 research and innovation programme under grant agreement No. 727550, and by the Mexican Energy Sustainability Fund CONACYT-SENER, Project 2015-04-268074. More information can be found on the GEMex Website: http://www.gemex-h2020.eu.

INTRODUCTION

Acoculco is a high temperature geothermal system within a Pliocene-Pleistocene volcanic complex. Two wells have been drilled showing temperatures above 300°C at depths below 1800 m, but very limited permeability. Acoculco is considered as a candidate for the application of EGS technologies.

Therefore, the Acoculco field was explored extensively with various geoscientific methods, including geophysics, within the frame of the GEMex Project. Resistivity data; MagnetoTelluric data (MT) and co-located Transient ElectoMagnetic data (TEM), were collected during several campaigns in Acoculco from early November 2017 until February 2019. The field campaign was run by UNAM (National Autonomous University of Mexico) together with UMSNH (Michoacan University of Saint Nicholas of Hidalgo, Mexico) and Cisese (Ensenada Centre for Scientific Research and Higher Education, Mexico). ÍSOR (Iceland GeoSurvey) and KIT (Karlsruhe Institute of Technology, Germany) from the European consortium participated in the campaign in the beginning and were a part of the discussions and decisions taken on appropriate field practices and the resistivity survey in general. The campaign took longer than anticipated due to unforeseeable problems of different kinds that came up during the acquisition period. However, almost all the data originally planned to collect were collected. Most of the data are high quality data. A similar survey was conducted in the close by superhot geothermal system, Los Humeros (Benediktsdóttir et al., 2020).

A resistivity model of the Acoculco survey area has been compiled from the results of 1D joint inversion of the TEM and MT data. It is based on inversion of the TEM data and the apparent resistivity and phase calculated from the determinant value of the MT impedance tensor. During the inversion process the MT data were static shift corrected using the TEM data.

Here data acquisition, processing and 1D inversion of the MT/TEM data from the Acoculco area is discussed. Phase tensor analyses from the area is presented in Held et al. (2020) and sensitivity study of 3D inversion of MT data from Acoculco is presented in Ruiz-Aguilar et al. (2020).

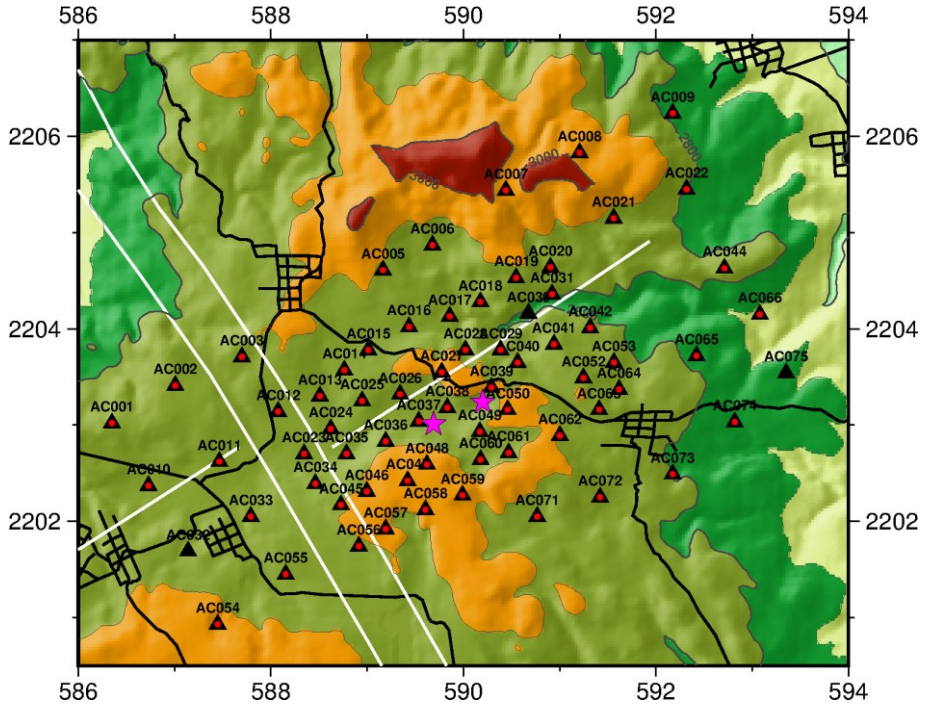

Figure 1: Location map for the Acoculco survey area. Black triangles and red circles denote the location of MT and TEM soundings, respectively. Purple stars are the two wells, white lines are major faults in the area and black lines are roads. Coordinate system is UTM zone 14 WGS84.

DATA ACQUISITION

The survey in Acoculco was not a conventional resistivity survey, its aim was first and foremost to facilitate the application of EGS technologies. Results from geological mapping were used for MT/TEM site locations. The sites were arranged on a grid with 400 m spacing for the fine grid and 800 m spacing for the coarser grid, with an orientation parallel and perpendicular to the main geological strikes (see Figure 1). In Acoculco 68 MT and 65 TEM soundings were measured, some of the planned sites were not accessible and some adjustments to the plan had to be made during the acquisition.

In the MT method, the natural fluctuations of the Earth's magnetic field are used as signal source. Those fluctuations induce currents in the ground which are measured in the surface (E_x and E_y). The magnetic field is measured in three orthogonal directions (H_x, H_y and H_z). It is customary to have the x-direction to the magnetic north and that was done in Acoculco. For a homogeneous or layered Earth, the electrical field is induced by (coherent with) its orthogonal source magnetic field (i.e. E_x correlates with H_y, and E_y with H_x). For more complicated resistivity structures these relations become more complex.

The short-period MT data (high frequency) mainly reflect the shallow structures due to their little depth of penetration, whereas the long period data mainly reflect the deeper structures. The MT method has the greatest exploration depth of all resistivity methods, some tens of kilometers, depending on the recorded periods, and is practically the only method for studying deep resistivity structures. In this survey, the exploration depth of the MT soundings is around 3-10 km but varied considerably depending on resistivity and in particular on data quality.

The magnetic field was measured with induction coils and the electrical field by a pair of sealed $PbPbCl_2$ type electrodes. The electrical dipole length was typically 90 m.

The measured MT time series are Fourier transformed into the frequency domain and the "best" solution that describes the relation between the electrical and magnetic field is found by assuming the following equation:

$$\begin{bmatrix} E_x \\ E_y \end{bmatrix} = \begin{bmatrix} Z_{xx} & Z_{xy} \\ Z_{yx} & Z_{yy} \end{bmatrix} \begin{bmatrix} H_x \\ H_y \end{bmatrix}$$

Or in matrix notation: $\vec{\boldsymbol{E}} = \boldsymbol{Z}\vec{\boldsymbol{H}}$

Where, $\vec{\boldsymbol{E}}$ and $\vec{\boldsymbol{H}}$ are the electrical and magnetic field vectors (in the frequency domain), respectively, and $\mathbf{Z}$ is a complex impedance tensor which contains information on the subsurface resistivity structure.

The tensor elements are found by minimizing the absolute square of the difference between the left and the right-hand side of the equation above with respect to the tensor elements.

For a homogeneous and layered (1D) Earth $Z_{xy} = -Z_{yx}$ and $Z_{xx} = Z_{yy} = 0$. For a 2D Earth, i.e. resistivity varies with depth and in one of the two principal horizontal directions, it is possible to rotate the coordinate system such that $Z_{xx}= Z_{yy}= 0$, but $Z_{xy} \neq -Z_{yx}$. For a 3D Earth all the impedance tensor elements are different.

From the impedances, apparent resistivity (ρ) and phases (θ) for each frequency are calculated as:

$$\rho_{xy} = 0.2T\left|Z_{xy}\right|^2;\ \theta_{xy} = \arg\left(Z_{xy}\right)$$

$$\rho_{yx} = 0.2T\left|Z_{yx}\right|^2;\ \theta_{yx} = \arg\left(Z_{yx}\right)$$

In the field work five sets of MT equipment from Metronix, ADU-07 type, were used, collecting data in the frequency range from 0.0001 Hz to 10 kHz. The sampling frequency was 4096 Hz for 30 minutes and 128 Hz for at least 20 hours. One of the MT stations served as a reference station, measuring a continuous MT signal, located 80 kilometers away in Los Humeros. This recording was used as reference signal to give better data quality (see e.g. Gamble et al., 1979). Some of the MT sounding data were of low quality, mainly due to noise originating from the proximity of power lines.

The main purpose of the TEM survey was to correct for the static shift of the MT data. The static shift is caused by near-surface resistivity in-homogeneities at the sounding site and/or topography which distorts the electric field measured in the surface. Static shift introduces an unknown shift multiplier, S, (shift on log-scale) of the apparent resistivity. The shift multiplier is practically independent of frequency (period), therefore, the whole apparent resistivity curve can be shifted up or down when plotted on log-scale (Árnason, 2015).

The equipment used for the TEM measurements was a TerraTEM equipment from Monex GeoScope; single loop, i.e. the same loop was used for transmitting and receiving. The loop size was 100 m x 100 m and the injected current around 8 A. The frequency was 30 Hz, 10 Hz and 2.5 Hz.

DATA PROCESSING

The MT data from the survey area were processed and quality controlled. ProcMT was used for quality check during fieldwork and the Bounded Influence Remote Reference Processing method, BIRRP (Chave and Thomson, 2004) for transfer functions robust estimation.

To increase the quality of interpretable data the following processing schemes were tested intensively: 1) Robust processing scheme using Egert and Booker (1986); 2) Robust processing scheme using Chave and Thomson (2004); and 3) Processing scheme implemented in WinGLink Software (© Schlumberger). WinGLink Software processing yielded data of insufficient quality. After quality analysis of a variety of stations considering the whole frequency range, the strongest reduction of uncertainties, the optimal elimination of noise and the generation of smooth curves was achieved using the BIRRP code. The code was used in advanced mode considering remote referencing. To increase the penetration depth, the processed frequency range was enlarged by decimation of the measured 128 Hz data to 4 Hz and subsequent processing of three frequencies bands (4096 Hz, 128 Hz and 4 Hz).

ELECTRICAL STRIKE ANALYSIS

Electrical strike is often associated with geological faults and fractures, not necessarily seen on the surface. Analysis of the strike can give further information on the subsurface structure and support the resistivity model (see e.g. Hersir et al., 2019).

Vertical magnetic field data, the H_z component, are frequently used for directional analysis through the so-called Tipper, $\boldsymbol{T}$, which relates the vertical component of the magnetic field to its horizontal components:

$$\boldsymbol{H}_z = T_x\boldsymbol{H}_x + T_y\boldsymbol{H}_y$$

T_x and T_y are the x- and y-component of the Tipper, respectively. For 1D Earth, the Tipper is zero, $T_x = T_y = 0$. For a 2D Earth, the coordinate system can be rotated so that the x-axis is in the strike direction, the so-called Tstrike, i.e. $T_x = 0$, but $T_y \neq 0$. This is done by minimizing $|T_x|$.

The Tipper can be represented as the real and imaginary parts of the x -and y-components in the form of induction arrows (Figure 2 and 3). According to the sign convention used here (the Wiese convention (Wiese, 1962)), the real arrows point away from a zone of low resistivity and towards a zone of higher resistivity (Berdichevsky and Dmitriev, 2002). The length of the arrows indicates the size of the resistivity contrast. For 2D Earth, the real and imaginary arrows are collinear, pointing in opposite directions perpendicular to the electrical strike (Berdichevsky and Dmitriev, 2002).

Figure 2 and 3 present the results of the strike analyses for the Acoculco survey area. They show the induction arrows and Tstrike at each survey point in the period band, 0.1 s – 1 s and 1 s – 10 s, respectively. These period bands correspond to a depth of a few hundred metres to a few kilometres, respectively.

The real part of the induction arrows at 0.5 s (Figure 2) for soundings located in the centre of the survey area, show a preferred orientation toward a location near the western well, suggesting the presence of a resistive body at that location. The Tstrike in the period range 0.1 s – 1 s (Figure 2) is scattered, although some patterns can be seen. Many of the soundings exhibit a preferred SW-NE orientation, along one of the main faults in the area while preferred orientation at other soundings seem to fall in line with the other fault trend in the area, SE-NW.

The length of the real part of the induction arrows at 5 s (Figure 3) is small, suggesting a 1D Earth. Note that in some cases, for soundings located in the outskirts of the survey area, the length of the real part of the indcution arrow is large. This is either due to some local effects in the structure but, more likely, due to noisy Tipper data. The Tstrike in the period range 1 s – 10 s (Figure 3) is very scattered for soundings in the western part of the survey area, where no preferred orientation seems to be present. For soundings located to the east of the eastern well the preferred direction seems to be NNW-SSE and NE-SW for soundings located south and north of the SW-NE fault, respectively.

Acoculco can be divided into two parts. The soundings to the east exhibit a NS preferred orientation according to the Tstrike for all frequencies. The electrical strike in Acoculco is discussed further through the phase tensor analyses in Held et al. (2020).

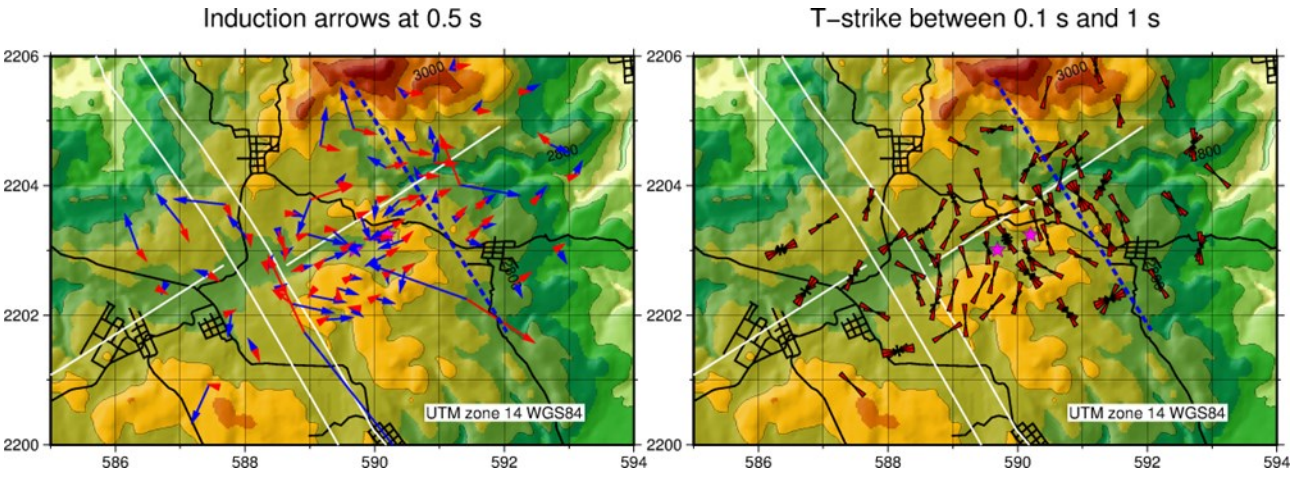

Figure 2. Induction arrows at 0.5 s, at each sounding in the Acoculco area; blue and red arrows are the real and imaginary components, respectively (left panel). Tstrike between 0.1 s – 1 s, at each sounding in the Acoculco area (right panel). The white lines are faults in the area and black lines are roads. Two magenta filled stars are the location of the two wells. The blue dashed line divides the area into two parts. The coordinate system used is UTM zone 14 WGS84.

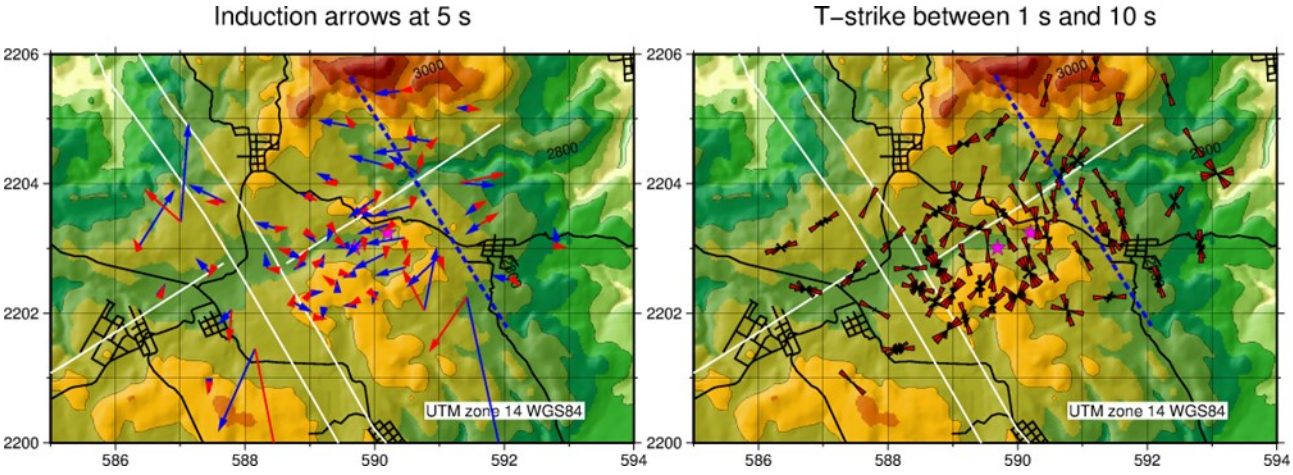

Figure 3. Induction arrows at 5 s, at each sounding, in the Acoculco area; blue and red arrows are the real and imaginary components, respectively (left panel). Tstrike between 1 s – 10 s, at each sounding in the Acoculco area (right panel). The white lines are faults in the area and black lines are roads. Two magenta filled stars are the locations of the two wells. The blue dashed line divides the area into two parts. The coordinate system used is UTM zone 14 WGS84.

1D JOINT INVERSION USING TEMTD

In 1D inversion of MT data it is customary to invert for one of the three rotational invariant parameters:

$$Z_{av} = \frac{Z_{xy} - Z_{yx}}{2}$$

$$Z_{det} = \sqrt{Z_{xx}Z_{yyY} - Z_{xy}Z_{yx}}$$

$$Z_{gm} = \sqrt{-Z_{xy}Z_{yx}}$$

All these parameters give the same values for a 1D Earth response, for a 2D Earth the *det* (determinant) and the *gm* (geometric mean) reduce to the same value but the *av* (arithmetic mean) is different. For a 3D response, all these parameters are different.

There are different opinions on which of the three invariants, if any, is best suited for 1D inversion. However, based on comparison of model responses for 2D and 3D models, it has been suggested that the determinant invariant is the one to use (see e.g. Park and Livelybrook, 1989) and that was done for the data presented here.

The 1D inversion was done by using the TEMTD code (Árnason, 2006). Apparent resistivity and phase, calculated from the determinant of the MT impedance tensor were inverted jointly with TEM data. In the joint TEM/MT inversion, a static shift parameter is obtained; the TEM data are used to shift the MT apparent resistivity curve up (shift multiplier S < 1), or down (shift multiplier S > 1), see Figure 4.

Occam (minimum structure) inversion (Constable et al., 1987) was used with 100 horizonal layers. In the Occam inversion the thicknesses of the layers are kept fixed and they grow exponentially with depth until they reach a homogeneous half-space. With this parametrization the structure is minimized, and the resistivity varies smoothly with depth. The parameters inverted for are the resistivity values of each layer and the shift multiplier S. Inversion parameters (e.g. the bottom to the homogeneous half-space and initial model) are varied from one sounding to another depending on the data.

When all sounding pairs have been inverted, the resulting 1D models are interpolated in space to form a one “pseudo” 3D model. The results are presented in the forms of horizontal and vertical cross-sections of the model.

Figure 1 shows the location of the resistivity soundings in the Acoculco survey area used in the 1D inversion. A total of 65 MT/TEM sounding pairs were 1D jointly inverted and 1 MT soundings with no co-located TEM data. In that case the TEM data were of bad quality and the shift was assumed to be 1. Figure 4 shows examples of inverted MT/TEM pair (Figure 4A) and where only MT data were available (Figure 4B).

RESISTIVITY STRUCTURE OF HIGH TEMPERATURE GEOTHERMAL FIELDS

The subsurface resistivity structure of high temperature geothermal fields in volcanic environment is broadly similar and depends mostly on hydrothermal alteration (Árnason et al., 1987; Árnason et al., 2000; Ussher, 2000; Flóvenz et al., 2012; Lévy et al., 2018). The relationship between subsurface resistivity, hydrothermal alteration, temperature and conduction mechanism is summarized in Figure 5. Close to the surface the resistivity is high, reflecting unaltered rock – with pore fluid conduction. Below the high resistivity, a low resistivity cap is found consisting of rocks with considerable amount of conductive alteration minerals, like smectite that has hydrated and loosely bound cations, and high Cation Exchange Capacity (CEC) which makes the minerals conductive (Lévy et al., 2018) – with surface conduction in clay minerals. The resistivity of the cap decreases with temperature until a core of high resistivity is reached. The transition from the low resistivity cap to the high resistivity core coincides with a change in mineral alteration, i.e. from the high CEC smectite to the low CEC mixed-layered clays, chlorite and epidote – with surface and pore fluid conduction. CEC within hydrothermal systems and its relation to the alteration mineralogy and electrical resistivity based on CEC measurements in several high temperature wells in Iceland is discussed in Weisenberger et al. (2019).

Formation of alteration minerals depends on temperature, primary minerals and the chemical composition of the geothermal fluid. Hydrothermal alteration begins at 50-100°C and the change from smectite to chlorite type alteration assemblage occurs at temperatures close to 230°C. If the temperature that produced the alteration mineralogy prevails, the resistivity structure can be used to predict temperature. But if cooling takes place, the alteration remains and so does the resistivity structure. The resistivity structure can, therefore, in most cases be regarded as a “maximum thermometer”. It has happened that alteration minerals have indicated lower temperature than measured in the wells. This has been interpreted as a young system being heated up and the alteration is lagging behind, still not in equilibrium with the temperature (Hersir and Árnason, 2009; Flóvenz et al., 2012).

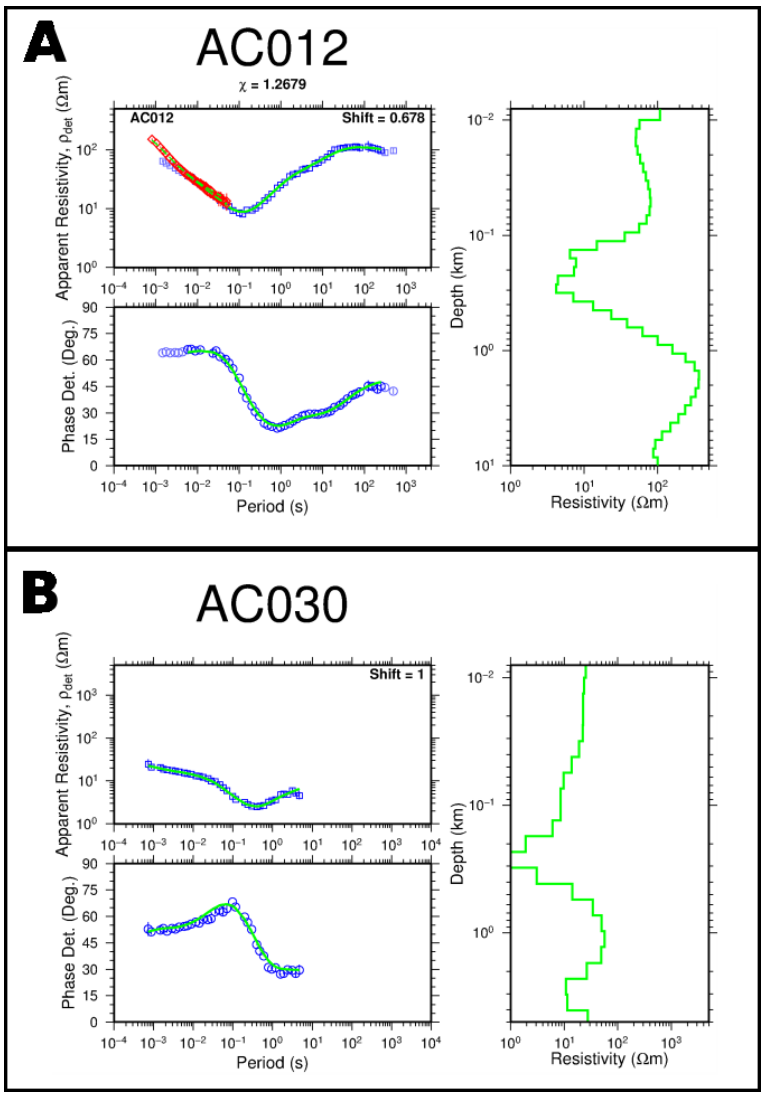

Figure 4: Examples of inverted resistivity determinant data. In both A and B, the upper left panel is MT resistivity data (in blue) and for A only, the upper left panel is the apparent resistivity of TEM data transformed to a pseudo curve (red points). The green curve is the response of the model shown in the right panel. The lower left panel is the phase of the MT data (blue circles) and the green curve is the MT phase response of the model shown in the right panel. A: Inversion of sounding AC012 where MT and TEM data were inverted jointly. The static shift multiplier is shown in the upper right hand corner of the upper left panel (0.678). B: Inversion of sounding AC030 where only MT data were available. For location of the soundings, see Figure 1.

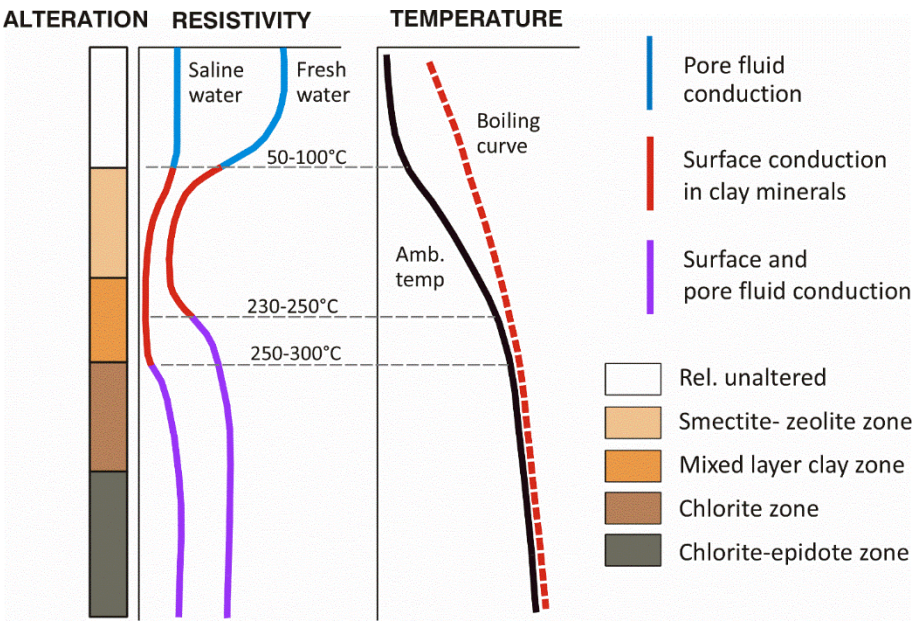

Figure 5. The general resistivity structure and alteration of the basaltic crust in Iceland summarized in Flóvenz et al. (2012); modified from Flóvenz et al. (2005).

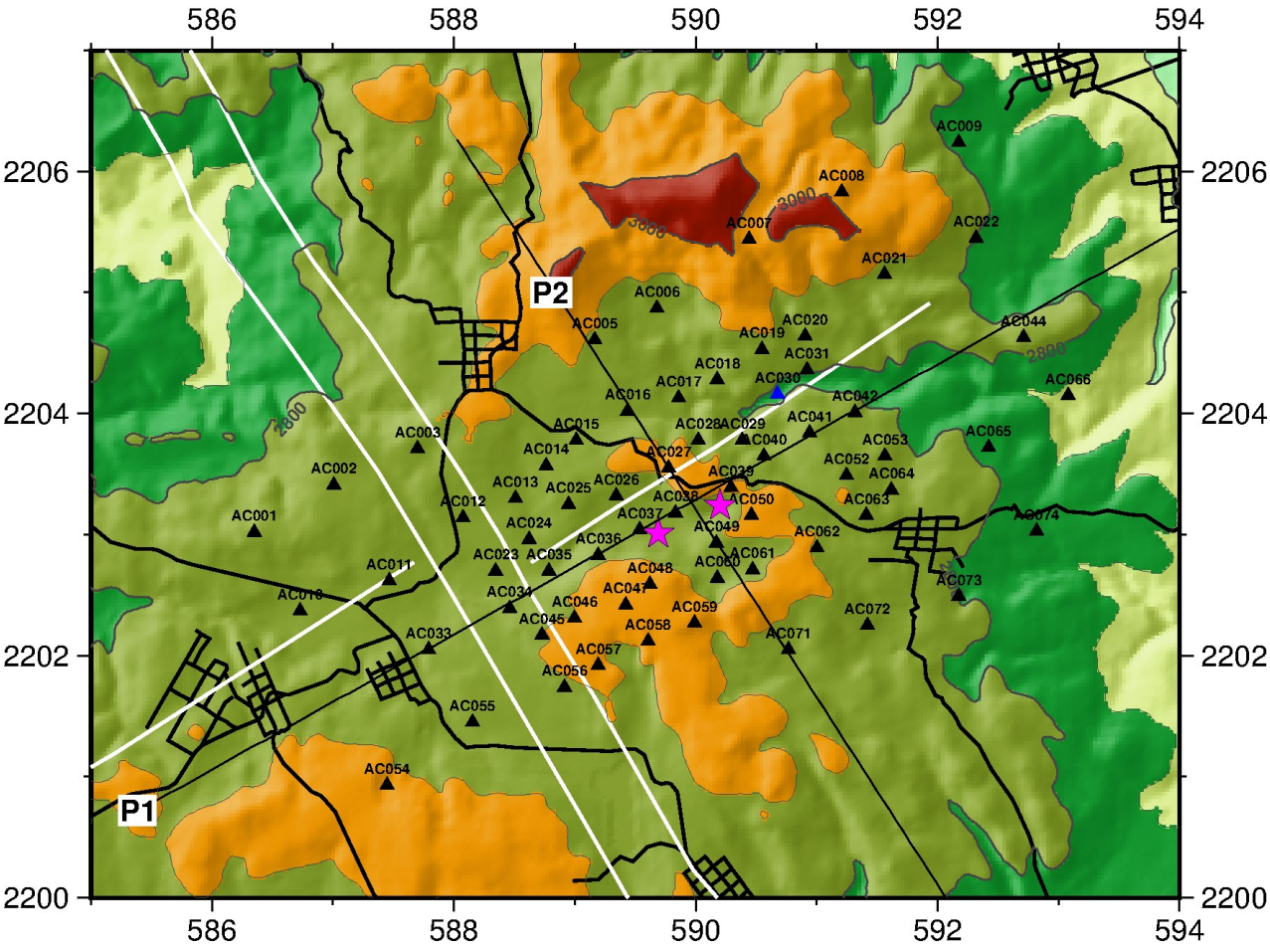

Figure 6: Location map of the Acoculco area. The triangles are the sounding location with (black) and without (blue) TEM data. Purple stars are the two wells, thick lines are roads and white lines are major faults in the area. The thin black lines are location of vertical sections, P1 and P2 through the resistivity model.

RESULTS

Figure 7 shows horizontal cross-sections through the "pseudo" 3D resistivity model at four different depths. At 2700 meters above sea level (Figure 7A) the low resistivity clay cap is clearly seen in the NW part of the survey area. At 2500 meters above sea level (Figure 7B) the low resistivity clay cap is now seen in the NE part of the survey area while intermediate values are present below where the low resistivity cap is present at 2700 meters above sea level. The highest resistivity values are around the western well, that is surrounded by zones of lower resistivity, indicating that this is the location of the up doming resistive core. A transition zone in the resistivity structure was identified (see Figure 2 and 3) and to the northeast low resistivity values are present.

At 1500 meters above sea level (Figure 7C) the area to the southwest of the transition zone exhibits high resistivity values but the area to the northeast is characterized by intermediate values. In the area between 1500 meters above sea level down to 3000 meters above sea level (Figure 7D) the resistivity structure remains similar.

Figure 8 and 9 shows two vertical cross-sections through the "pseudo" 3D resistivity model down to sea level and to 5 km depth below sea level. Their location is given in Figure 6.

Profile 1 on Figure 8 shows a SW-NE lying cross-section through the model. The low resistivity cap is thick towards the edges of the profile but gets a little thinner towards the centre below soundings AC035-AC039. The resistive core clearly domes up, symmetrically, underneath the centre of the area below sounding AC037, which is located close to the westernmost well.

Profile 2 on Figure 9 shows a NW-SE lying vertical cross-section through the model. The resistivity structure is characterized by a low resistivity cap and a resistive core below. The doming up of this structure is not a evident as for Profile 1. At depth, a layer of intermediate resistivity is present between 1000 – 5000 meters below sea level, which is cut by a column of a higher resistive located directly under the area between soundings AC027 and AC049.

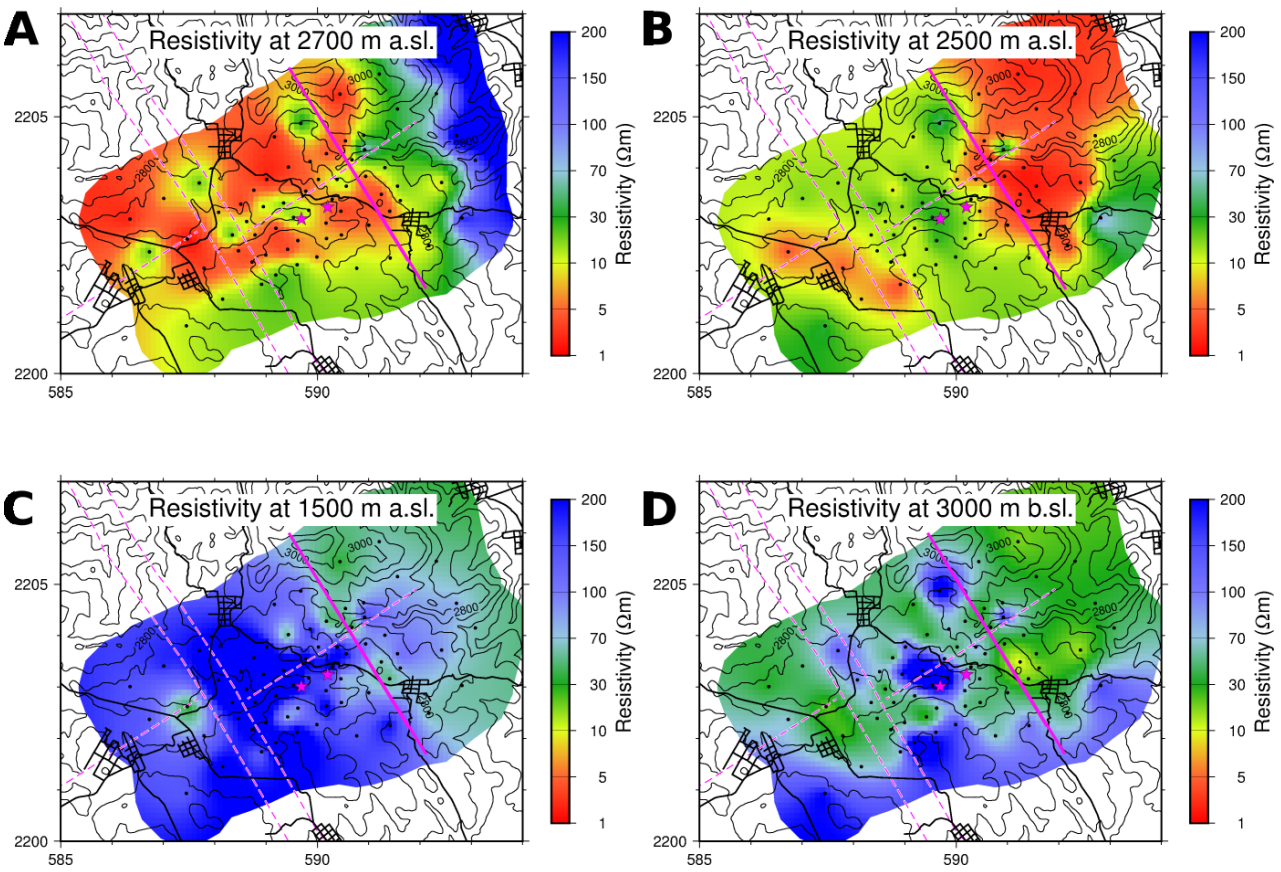

Figure 7: Horizontal cross-sections through the "pseudo" 3D resistivity model of the Acoculco area at 2700 meters above sea level (A), 2500 meters above sea level (B), 1500 meters above sea level (C) and 3000 meters below sea level (D). Thick black lines are roads, thin black lines are elevation contours every 50 meters. Pink stars are the locations of the two wells, dashed pink lines are major fault lines and thick pink line is the discontinuity as observed from the resistivity data (see Figure 2 and 3).

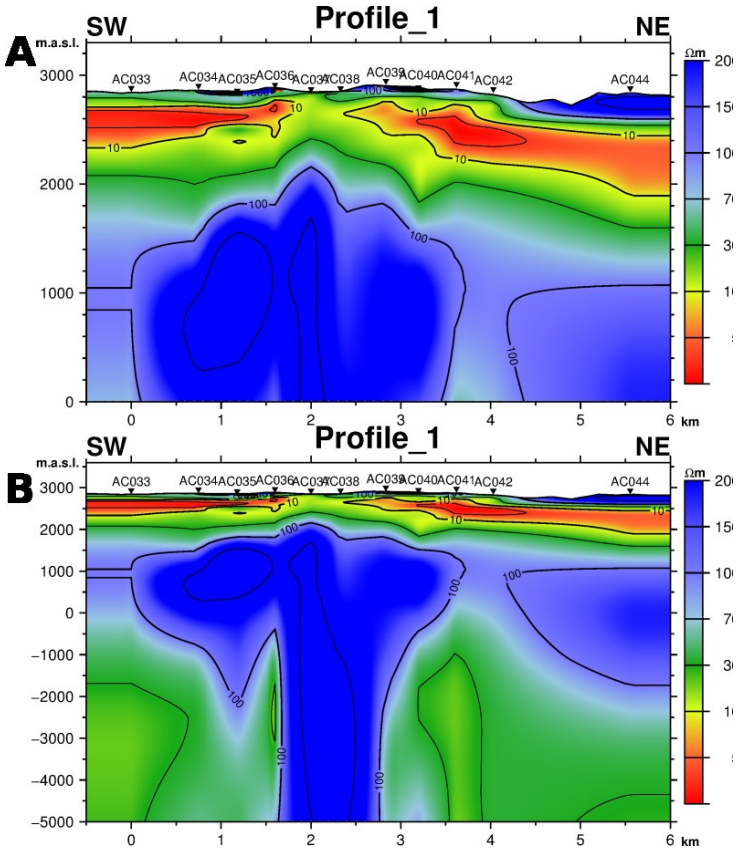

Figure 8: Resistivity Profile 1: SW-NE lying vertical cross-section through the "pseudo" 3D resistivity model of the Acoculco area down to sea level (A) and 5000 meters below sea level (B). Triangles at the surface are the sounding locations and their names. The location of the profile is shown on Figure 6.

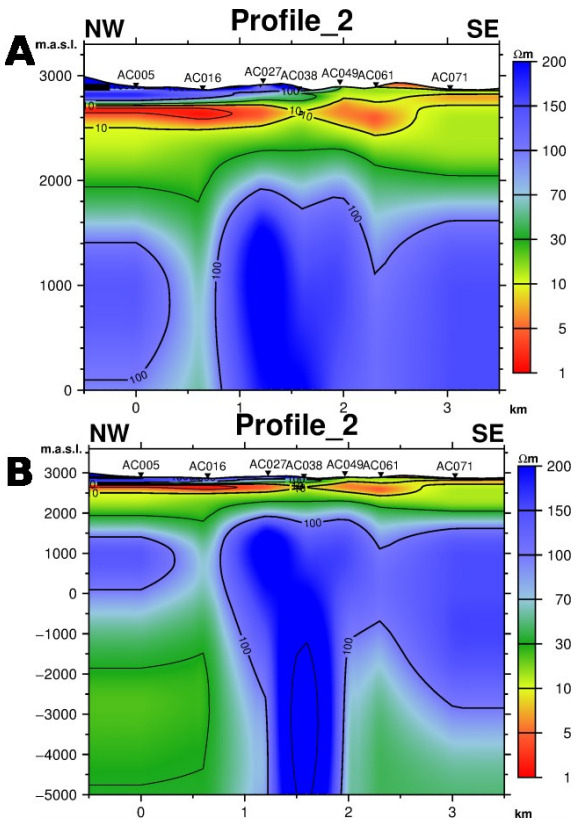

Figure 9: Resistivity Profile 2: NW-SE lying vertical cross-section through the "pseudo" 3D resistivity model of the Acoculco area down to sea level (A) and 5000 meters below sea level (B). Triangles at the surface are the sounding locations and their names. The location of the profile is shown on Figure 6.

CONCLUSIONS

In the Acoculco survey area, the "pseudo" 3D resistivity model from 1D inversion exhibits mostly one-dimensional resistivity structure. The area explored is divided into two areas that can be distinguished from one another, the boundary could well be a buried fault. The low resistivity cap (presumably reflecting smectite hydrothermal alteration) becomes thinner close to the western well. It is in this area where the resistive core (presumably reflecting chlorite/epidote hydrothermal alteration) is the shallowest in a very confined area, suggesting the existence of a zone of geothermal interest. A 3D inversion has been performed for the full impedance tensor of the static shift corrected MT data using different initial models. Two codes were applied for comparison, the WSINV3DMT code was run in Europe and ModEM in Mexico. The results will be published later together with comparison with other geoscientific results.

REFERENCES

Árnason, K., 2006. TEMTD a program for 1D inversion of TEM and MT data. Short manual. ISOR internal report, 17 pp.

Árnason, K., 2015: The static shift problem in MT soundings. In: Proceedings of the World Geothermal Congress 2015, Melbourne, Australia, 19-25.

Árnason, K., Flóvenz, Ó., Georgsson, L.S., and Hersir, G.P., 1987. Resistivity structure of high temperature geothermal systems in Iceland. International Union of Geodesy and Geophysics (IUGG) XIX General Assembly, Vancouver, Canada, Abstracts V, 477.

Árnason, K., Karlsdóttir, R., Eysteinsson, H., Flóvenz, Ó.G. and Gudlaugsson, S.Th., 2000. The resistivity structure of high-temperature geothermal systems in Iceland. In: Proceedings of the of the World Geothermal Congress 2000, Kyushu-Tohoku, Japan, 923–928.

Benediktsdóttir, Á., Arango-Galván, C., Hersir, G.P., Held, S., Romo Jones, J.M., Salas, J.L., Aviles, T., Aquilar, D.R., Vilhjálmsson, A.M., Manzella, A. and Santilano, A., 2020. The Los Humeros Superhot Geothermal Resource in Mexico: Resistivity Survey (TEM and MT); Data Acquisition, Processing and Inversion – Geological Significance. In: Proceedings of the World Geothermal Congress 2020 Reykjavík, Iceland.

Berdichevsky, M.N. and Dmitriev, V.I., 2002. Magnetotellurics in the context of the theory of ill-posed problems. Society of Exploration Geophysicists, 215 pp.

Chave, A. D., and Thomson, D. J., 2004. Bounded influence magnetotelluric response function estimation. Geophys. J. Int., 157, 988-1006.

Constable, C.S., Parker, R.L. and Constable, C.G., 1987. Occam's inversion: a practical algorithm for generating smooth models from electromagnetic sounding data, Geophysics, 52, 289-300.

Egbert, G. and Booker, J., 1986. Robust estimation of geomagnetic transfer functions, Geophys. J. Int., 173–194.

Flóvenz, Ó.G., Spangenberg, E., Kulenkampff, J., Árnason, K., Karlsdóttir, R., and Huenges, E., 2005. The role of electrical conduction in geothermal exploration. In: Proceedings of the World Geothermal Congress 2005 Antalya, Turkey.

Flóvenz, Ó.G., Hersir, G.P., Saemundsson, K., Ármannsson, H. and Fridriksson, Th., 2012. Geothermal Energy Exploration Techniques. In: Sayigh, A., (ed.) Comprehensive renewable energy, Volume 7. Elsevier, Oxford, 51-95.

Gamble, T. D., Goubau, W. M., and Clarke, J., 1979. Magnetotellurics with a remote magnetic reference. Geophysics, 44, 53-68.

Held, S., Benediktsdóttir, Á., Arango-Galván, C., Hersir, G.P., Romo Jones, J.M., Cornjeco, N., Salas, J.L., Aviles, T., Brogi, A., Vilhjálmsson, A.M., and Schill, E., 2020. The Los Humeros and Acoculco Geothermal Resources in the Trans-Mexican Voclanic Belt: Magnetotelluric Phase Tensor Analyses and its Significance for Tectonic Interpretation. In: Proceedings of the World Geothermal Congress 2020 Reykjavík, Iceland.

Hersir, G.P., and Árnason, K., 2009. Resistivity of rocks. Short Course on Surface exploration for Geothermal Resources, organized by UNU-GTP and LaGeo, in Ahuachapan and Santa Tecla, El Salvador. http://www.unugtp.is/en/moya/page/sc-09/.

Hersir, G.P., Árnason, K., Vilhjálmsson, A.M., Saemundsson, K., Ágústsdóttir, Th. and Friðleifsson, G., 2018. Krýsuvík high temperature geothermal area in SW Iceland: Geological setting and 3D inversion of magnetotelluric (MT) resistivity data. Journal of Volcanology and Geothermal Research. https://doi.org/10.1016/j.jvolgeores.2018.11.021.

Lévy, L., Gibert, B., Sigmundsson, F., Flóvenz, Ó., Hersir, G., Briole, P. and Pezard, P., 2018: The role of smectites in the electrical conductivity of active hydrothermal systems: electrical properties of core samples from Krafla volcano, Iceland. Geophysical Journal International, Volume 215, Issue 3, 1558-1582. https:doi.org/10.1093/gii/ggy341.

Park, S. K. and Livelybrook, D. W., 1989. Quantitative interpretation of rotationally invariant parameters in magnetotellurics. Geophysics, 54, 1483–1490.

Ruiz-Aguilar, D., Benediktsdóttir, Á., Vilhjálmsson, A.M., Arango-Galván, C., Hersir, G.P., and Romo-Jones, J.M., 2020. Different Strategies Applied to 3D Inversion of MT data from Los Humeros Superhot Geothermal Resource in Mexico-H2020 GEMex Project. In: Proceedings of the World Geothermal Congress 2020 Reykjavík, Iceland.

Ussher, G., Harvey, C., Johnstone, R., and Anderson, E., 2000. Understanding the Resistivities Observed in geothermal Systems. In: Proceedings of the World Geothermal Congress 2000 Kyushu-Tohoku, Japan, 1915-1920.

Weisenberger, T.B., Ingimarsson, H., Hersir, G.P. and Flóvenz, Ó.G., 2019. Cation-exchange capacity within hydrothermal systems and its relation to the alteration mineralogy and electrical resistivity. Unpublished manuscript.

Wiese, H., 1962. Geomagnetische Tiefentellurik Teil II: Die Streichrichtung der untergrundstrukturen des elektrischen Widerstandes, erschlossen aus geomagnetischen Variationen. Geofisica pura e applicata, 52, issue 1, 83–103.